ISSN 1027-5495. Functional Materials, 28, No.2 (2021), p. 327-335.
doi:https://doi.org/10.15407/fm28.02.327

Simplified π-electron Green's function coupled-cluster computations: Applications to conjugated nanomolecules

A.V.Luzanov

STC "Institute for Single Crystals", National Academy of Sciences of Ukraine, 60 Lenin Ave., 61001 Kharkiv, Ukraine

Received August 12, 2020

The inclusion of electron correlation into large-molecule calculations is particularly vital for practical aspects of the Green's function (GF) theory. In the present paper, simple computational schemes of GF are given within the π-electron coupled cluster (CC) theory. In particular, the conventional LCCD method is modified by introducing a renormalized particle-hole correlation interaction, that lead us to a new more reliable scheme LCCD2. In the latter, the correlation interaction matrix contains easily computable additional terms which are quadratic in particle-hole amplitudes. The proposed models are tested for small systems. Selected examples for sufficiently large conjugated networks of helicene, graphene, and nanotube types are investigated by LCCD2 with a stress on long-range effects describing interactions of far-distant π-electron sites.

Keywords: Green's functions, conjugated hydrocarbons, π-electron correlations, extended quasi-correlation approach, LCCD, and LCCD2 models.

Спрощені обчислення π-електронної гринівської функції в схемі зв'язаних кластерів. Застосування до супряжених наномолекул. *А.В.Лузанов*

Включення ефектів електронної кореляції у розрахунки великих молекул є принциповим у практичних застосуваннях теорії гринівської функції (GF). У даній статті надано прості схеми обчислювання GF в межах π-електронної теорії зів'язаних кластерів (рмалізованої частинково-діркової кореляційної взаємодії, що веде до нової більш надійної схеми LCCD2. В останній матриця кореляційної взаємодії містить просто обчислювані додаткові члени, що є квадратичними щодо частинково-діркових амплітуд. Запропоновані моделі протестовано на малих системах. За методом LCCD2 досліджено окремі приклади досить великих супряжених структур за типом гелицена, графена та нанотрубки з акцентуванням на ефекти дальнодії, котрі описують взаємодію віддалених π-електронних центрів.

Включение эффектов электронной корреляции при расчете больших молекул является принципиальным в практических применениях теории гриновской функции (GF). В данной статье даны простые схемы вычислений GF в рамках π-электронной теории связанных кластеров (CC). В частности, модифицирована стандартная линейная схема LCCD при помощи перенормированного частично-дырочного корреляционного взаимодействия, что приводит к новой более надежной схеме LCCD2. В последней матрица корреляцийного взаимодействия содержит просто вычисляемые дополнительные члены, квадратичные по частично-дырочным амплитудам. Предложенные модели протестированы на малых задачах. По методу LCCD2 исследованы отдельные примеры довольно больших сопряженных структур типа гелицена, графена и нанотрубки с акцентом на эффекты дальнодействия, описывающие взаимодействие отдаленных π-электронных центров.

1. Introduction

Nowadays the theoretical principles of single-molecule electronics (SME) are more or less established (e.g., see [1–3]), and main efforts are directed to specific molecular systems which may have potential in a future nanoscale engineering. Recall that the key tool for understanding electron transport phenomena is the retarded one-electron Green's function (GF) theory. In the case of the SME problems, computations of molecular conductance are frequently made by using GF at the DFT (density functional theory) level. However, some principal deficiencies of DFT are reported in the SME context [2, 4, 5]. Another popular approach is using the simplest tight-binding (TB) model, or the Huckel method, for π-electron subshells (see review [6]). The latter produce a major contribution to the electron transport through conjugated hydrocarbons and other typical SME networks. Nonetheless, the full ignorance of long-distance and electron correlation effects make the TB approach too crude and even erratic in many cases [7–9].

Recently we have proposed improved TB-like schemes [7, 8] along with a more sophisticated model [9] which is based on the well-known half-projected Hartree-Fock (HPHF) scheme. Nevertheless, for sufficiently large networks it is desirable to aditionally compare results of the proposed models with those from independent and more reliable approximations. As for the latter we adopt here the conventional electron-correlation models based on restricted configuration interaction (CI) and related couple cluster (CC) techniques. The main purpose of this paper is to develop easily workable CC schemes for calculating GF and other electronic properties of complex π-electron materials and compare the obtained results with those previously given in [7–9]. Furthermore, here we are expanding the scope of our studies to include three-dimensional π-conjugated nanostructures as well.

2. One-electron TB-like models for π-shells

To begin with, we will briefly sketch the generic simple π-models we deal with in the paper. In the notations adopted here the TB (Huckel) Hamiltonian, h^{TB}, of the given π-conjugated system is fully determined by an adjacency matrix of the associated molecular graph. We will work with the so-called alternant hydrocarbons related to bipartite graphs. In this case all carbon π-sites can be divided into two disjoint sets of, say, starred and unstarred sites, and there are no chemical bonds between the sites of the same set.

The adjacency matrix of bipartite graph can be always written as a skew-diagonal block matrix. Accordingly, the conventional representation of is of the form

$$h^{TB} = -\begin{pmatrix} 0 & B \\ B^{\mathrm{T}} & 0 \end{pmatrix} \qquad (1)$$

where block B is constructed from 1's for adjacent sites (bonded carbon atoms); other elements are 0's. This Hamiltonian is given here in units of the effective resonance integral β_{eff} [7]. The attractive feature of TB is the easiness with which one performs computations of the corresponding retarded Green's function matrix G_0^{TB} at the Fermi level. Namely, G_0^{TB} is the resolvent matrix for Eq. (1):

$$G_0^{\mathrm{TB}} = [(i0^{+})I - h^{\mathrm{TB}}]^{-1}, \qquad (2)$$

where $i0^{+}$ is an imaginary positive infinitesimal, and I the unity matrix.

To overcome the shortage of the TB approximation for GF, a rather elementary modification of TB was invoked in [8]. In this modification termed EQC (extended quasi-correlated) model, the different orbitals for different spins are introduced in a very simple way. When describing GF and molecular conductance, EQC demonstrates a clear superiority over our previous quasi-correlated TB (QCTB) model from [7] (and over TB, of course).

In works [7–9], the full CI (FCI) method for π-electrons was employed as the natural reference method when evaluating the accuracy of QCTB and EQC approximations for GF and density matrix in small-size systems. In the case of middle-size systems (where FCI is not accessible) we have applied the sufficiently accurate HPHF scheme mentioned in the introduction. By HPHF we could check reliability of the simple theories, QCTB and TB, for quite complex structures with a score and more atoms which are beyond the computational accessibility of FCI. And yet, for sufficiently large systems (say, more then fifty atoms) the HPHF computations may be less reliable as a consequence of size-inconsistency inherent to the HPHF model. This fact motivated us to explore another techniques based on the good-quality CC models which we consider below.

3. Using Koopmans-like approximation for CC models

There exist many good quality models based the second-order many-body perturbation (MP2) [10] and more sophisticated CC theories given in [11–13] (see also [14] and Refs. therein). Besides, within the CC theory a simple, reasonable approach can be developed by modeling molecular ionization potentials (IP) and electron affinities (EA) via an appropriate Koopmans's approximation (in fact, the frozen-core model) [15]. As we will show further later in the paper, the ensuing π-electron Green's functions at a generalized Koopmans level of theory are also of good quality, and this fact is one of the main results of our study here.

The approach we use is based on [15] where approximate π-electron CC calculations of IP were offered for singlet ground states of small conjugated hydrocarbons. Throughout the paper the total number of π-electrons is N, with N being even. Following [15], let us restrict to the conventional CCD model, that is CC with double-orbital substitutions (i.e., double excitations only). In this approximation one constructs the Koopmans-like Hermitian operator, $f^{(+)}$, which determines the IP spectrum within a frozen-core CCD level. This $f^{(+)}$ (f^{Koop} in terms of [15]) acts in the subspace of spin-free occupied MOs $|i\rangle$ ($1 \le i \le N/2$) with orbital energies ε_i (as usual, the Hartree-Fock ones). The $f^{(+)}$ matrix elements are of the easily computable form:

$$f_{ij}^{(+)} = \varepsilon_i \delta_{ij} + \frac{w_{ij}^{(+)} + w_{ji}^{(+)}}{2}, \tag{3}$$

where

$$w_{ij}^{(+)} = \sum_{k}^{occ} \sum_{a,b}^{vac} t_{ab,jk} \left\{ 2\langle ik|g|ab\rangle - \langle ki|g|ab\rangle \right\}, \tag{4}$$

and g is the two-electron Coulomb repulsion operator. Moreover, in Eq. (4) the standard notation $t_{ab,jk}$ is used for the CCD particle-hole amplitudes related to double excitations.

The required IP spectrum $\{I_u\}_{1 \le u \le N/2}$ is identified with a set of eigenvalues of matrix $-f^{+} = \|-f_{ij}^{Koop}\|_{1 \le i,j \le N/2}$. The eigenvectors $\{0|d_{ij}^{(+)}\rangle\}_{1 \le u \le N/2}$ of this matrix correspond to the so-called one-electron Dyson orbitals. As a result, the GF "positive" (i.e., hole) part, $G_0^{(+)}$, is constructed from these eigenvectors, as follows:

$$G_0^{(+)} = \sum_{1 \le u \le N/2} \frac{|d_u^{(+)}\rangle\langle d_u^{(+)}|}{i0^{+} + I_u}. \tag{5}$$

In fact, the above given expressions can be considered as a specific approximation to EOM (equation-of motion) CCD model for IP or more general IP-EOM-CCSD, that is the EOM-CC theory that involves both single (t_{aj}) and double ($t_{ab,jk}$) excitation amplitudes. More exactly, to obtain term $w_{ij}^{(+)}$, Eq. (4), one must neglect by 2hp amplitudes in the corresponding EOM-CC equation (8) from [12].

In a like manner we treat the GF "negative" (i.e., particle) part, $G_0^{(-)}$, that is closely related to the molecular EA spectrum. Let us define the appropriate matrix $f^{(-)}$ whose eigenvalues $\{A_\nu\}_{1 \le \nu \le m}$ determine the EA spectrum (m denotes a total number of virtual orbitals). The $f^{(-)}$ matrix elements are of the form

$$f_{ab}^{(-)} = \varepsilon_a \delta_{ab} + \frac{w_{ab}^{(-)} + w_{ba}^{(-)}}{2}, \tag{6}$$

where

$$w_{ab}^{(-)} = -\sum_{i,j}^{occ} \sum_{c}^{vac} t_{ac,kl} \left\{ 2\langle kl|g|bc\rangle - \langle lk|g|bc\rangle \right\}. \tag{7}$$

Then $G_0^{(-)}$ is computed from the $f^{(-)}$ spectrum, as follows:

$$G_0^{(-)} = \sum_{1 \le \nu \le m} \frac{|d_\nu^{(-)}\rangle\langle d_\nu^{(-)}|}{i0^{+} - A_\nu}, \tag{8}$$

with the relevant Dyson orbitals $\{|d_\nu^{(-)}\rangle\}_{1 \le \nu \le m}$ being a set of the m eigenvectors of $f^{(-)}$. Eq. (7) for $w_{ab}^{(-)}$ corresponds again to the usual EOM-CCD theory where one must neglect by 2ph amplitudes occurring, say, in Eq. (8) from [12]. Evidently, the full GF at the Fermi energy should be equal to

$$G_0 = G_0^{(+)} + G_0^{(-)}. \tag{9}$$

At this point, we would like to make one helpful observation concerning alternant π-systems (see Section 2 above). If one is interesting in GF at the Fermi level only, i.e. G_0, there is no need in computing $G_0^{(-)}$ for alternants because any correct π-model of G_0, Eq. (9), must obey an alternant symmetry requirement [16]. The last states that G_0 has the same skew-diagonal block form as h^{TB} in Eq. (1). Then, nonzero matrix elements of G_0 between π-orbitals of starred and unstarred sites are determined solely by the corresponding $G_0^{(+)}$ elements. It is essential that, when calculating G_0, the IP and EA spectra in Eqs. (5) and (8) are shifted by the Fermi energy.

4. Further simplifications and modifications

When dealing with large-scale computations, it is necessary to employ as simple as possible techniques that produce double excitation amplitudes $t_{ab,jk}$. Indeed, owing to a poor algorithmic scaling of typical high-order CC approaches, the latter frequently become impractical to treat large-scale systems even within semiempirical π-schemes [17]. Only within the MP2 theory we can apply a quite elementary expression:

$$t_{ab,jk}^{\mathrm{MP2}} = \langle ab|g|jk\rangle / (\varepsilon_j + \varepsilon_k - \varepsilon_a - \varepsilon_b), \quad (10)$$

and this MP2 option for constructing G_0 was applied long ago (e.g., see [12] and Refs. therein).

In principle, the well-known linearized CCD (LCCD) method, being quite feasible to run large-scale problems on inexpensive computers, offers better results than in MP2, and this approach will largely occupy us in the present paper. However, as a rule the LCCD and related LCCSD methods (when amplitudes t_{aj} are additionally included) overestimate π-electron correlation effects markedly (e.g. see Table 8 in [18]). This drawback can be weakened by one simple modification which we propose below.

Recall that the LCCD equations for double excitations amplitudes can be symbolically written as an operator relation for the 4-index amplitude matrix

$$t = \|t_{ab,jk}\|, \quad (11)$$

namely,

$$\Pi^{[2]}(t) + g_{corr} = 0. \quad (12)$$

Here, $\Pi^{[2]}$ is a superoperator acting in a space of t-type matrices (see [19] for detail), and

$$g_{corr} = \|\langle ab|g|jk\rangle\|. \quad (13)$$

In fact, a spectrum of $\Pi^{[2]}$ gives two-electron excitation energies within the CID scheme (CI with double orbital substitutions). Analyzing a two-electron problem in these terms, as done in the Appendix to this paper, we arrive to an unsophisticatedly extended LCCD model, namely the new scheme LCCD2. This approximation takes the form of the above Eqs. (11)–(13) with a simple nonlinear correction to g_{corr}, as follows:

$$\Pi^{[2]}(t) + g_{corr}^{(t)} = 0, \quad (14)$$

$$g_{corr}^{(t)} = g_{corr} - \mathrm{t}g t \quad (15)$$

(Eq. (A6) in the Appendix). Stress that LCCD2 cannot be gained directly from the full CCD method. In the latter one finds, among many other terms, the quadratic contribution $\mathrm{t}gt$, but with opposite (positive) sign. It is also clearly that we can use amplitudes (11) taken at the above LCCD2 level of theory to produce, via the basic Eqs. (3)–(8), Koopmans-like estimations of GF matrix (9). The GF matrix thus obtained will be denoted by G_0^{LCCD2}.

In addition to LCCD2, we suggest a more elementary version of the LCCD-like theory with using a modified approach to g_{corr}. In this approach, that will be termed the LCCDm method, we take a fixed $g_{corr}^{(t)}$, which is now independent of t. Namely, during the iterations for solving Eq. (14), $g_{corr}^{(t)}$ is computed from double excitations amplitudes at the MP2 level:

$$g_{corr}^{(t)} \equiv g_{corr} - t^{\mathrm{MP2}} g t^{\mathrm{MP2}} \quad (16)$$

(t^{MP2} matrix from Eq. (10)). In this case the computations become more easily to be performed owing to linearity of Eq. (14) in respect to t, and the needed iterations tend to be more easily converged.

Now we preliminarily demonstrate that the above schemes work well for generic π-electron systems. In our calculations we use for all conjugated π-systems the standard model geometry (regular squares and hexagons) and conventional π-electron parameters (the C–C bond resonance integral $\beta_0 = -2.4$ eV, two-electron Coulomb repulsion integrals $\|\gamma_{\mu\nu}\|$ due to Ohno etc.). As in [7], the effective resonance integral is taken to be $\beta_{eff} = \beta_0 - \gamma_{12}/2$, where γ_{12} is the Coulomb repulsion integral for π-AOs in the C–C π-bond; $\beta_{eff} = -6.17656$ eV in the adopted π-parameterzation scheme.

To assess the quality of models, we study the small-size representative structures given in Fig. 1. In the case of quinoid molecules **6** and **7** (cyclic systems with one

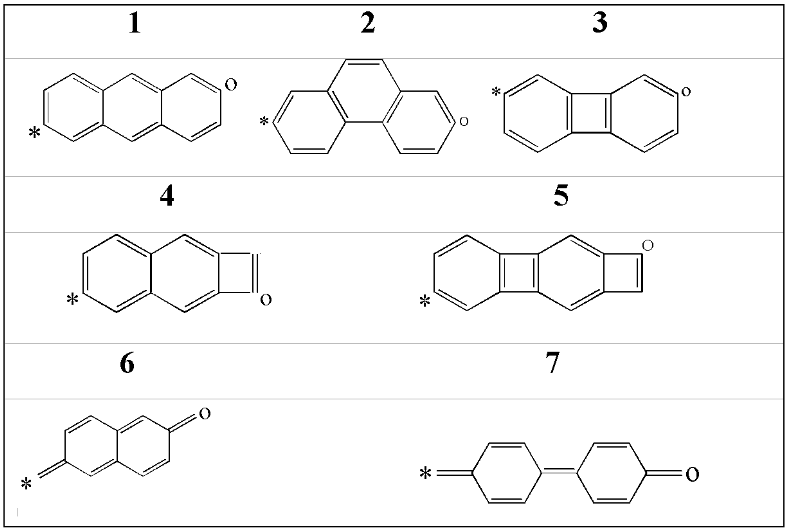

Fig. 1. Small conjugated molecules for testing CCD π-models. Asterisks and circles point out to the studied contact pairs (*, O).

Kekule structure) we employ alternating resonance integrals in the same manner as in [7].

With the above examples, we consider LCCD2 and other models in comparison with FCI. Recall that the latter is conventionally treated as the exact reference standard in the many-electron context. A suitable accuracy measure of electron-correlation models is usually defined in terms of the correlation energy, ε_{corr}, per electron, that is, the specific correlation energy $\bar{\varepsilon}_{corr} = \varepsilon_{corr}/N$. A close proximity of the given $\bar{\varepsilon}_{corr}$ to that of $\bar{\varepsilon}^{FCI}_{corr}$ provides a natural validity test of the given method. In Table 1, we collect relevant results for $\bar{\varepsilon}_{corr}$ in the π-systems of Fig. 1. We see that for all the systems of Fig. 1 our LCCD2 scheme is the most closest to the exact (FCI) π-theory. Along with this we notice that the LCCD2 computations by Eqs. (14) and (15) are in fact no more difficult than those in the LCCD case. Simultaneously, LCCD2 and LCCDm are much simpler than the conventional CCD method; the last, besides, underestimates $\bar{\varepsilon}_{corr}$ rather markedly.

Table 1. Specific π-electron correlation energy $\bar{\varepsilon}_{corr}$ (in eV) for conjugated hydrocarbons in various many-body theories. Bold-font integers refer to the calculated structures from Fig. 1

No	CCD	LCCD	LCCDm	LCCD2	FCI
1	0.1362	0.1433	0.1417	0.1409	0.1409
2	0.1296	0.1348	0.1333	0.1331	0.1336
3	0.1336	0.1388	0.1373	0.1371	0.1374
4	0.1460	0.1546	0.1530	0.1510	0.1506
5	0.1502	0.1639	0.1621	0.1581	0.1550
6	0.1652	0.1833	0. 1819	0.1747	0.1733
7	0.1641	0.1848	0.1833	0.1753	0.1735

5. Accuracy of approximate Green's functions for small π-systems

In this section we return to GF and report the numerical results for assessing accuracy of the Koopmans-like estimations for GF matrices in CCD and the new schemes LCCDm and LCCD2. To this end, we use a suitable statistical measure in the form of the relative (in respect to FCI) square-mean error (fluctuation), s_G. We supply this s_G with an additional upper affix, X, to distinguish the errors for different models. Explicitly, s_G^X is defined as follows:

$$s_G^X = \frac{\|G_0^X - G_0^{FCI}\|}{\|G_0^{FCI}\|}, \qquad (17)$$

where X specifies the used method, and $\| \ \|$ symbolizes taking Euclidean matrix norm. In Table 2 we present the obtained error data for X = TB, EQC, CCD, LCCDm and LCCD2. Note that as previously in [7–9], G_0^X for all X is expressed in units of $1/\beta_{eff}$.

From Table 2 we conclude that as a rule the EQC model of [8] turns out to be only slightly less accurate than the CC models (nothing to say about excessively crude TB

Table 2. Relative GF error s_G^X, Eq. (17), for various π-electron theories; X = TB, EQC, CCD, LCCD2 and LCCDm). Bold-font integers refer to the calculated structures from Fig. 1

No	TB	EQC	CCD	LCCDm	LCCD2
1	0.396	0.064	0.028	0.029	0.028
2	0.210	0.068	0.026	0.027	0.027
3	0.384	0.064	0.030	0.032	0.032
4	0.670	0.052	0.046	0.046	0.046
5	2.513	0.056	0.062	0.052	0.056
6	0.975	0.089	0.136	0.122	0.127
7	1.254	0.105	0.176	0.155	0.163

approach). Moreover, from Table 2 it appears that in fact LCCDm and LCCD2 give almost the same good results as the more consistent CCD approach. For strongly electron-correlated systems such as **5**÷**7**, LCCDm is even a bit better. At the same time, one should not forget the well-known fact that unsophisticated CC methods (LCCD, CCD, and similar class theories) as based on the single-determinant reference state, cannot be fully consistent for the systems with sufficiently strong electron correlation effects (e.g., large quinoid structures are just of this type).

Additional useful details can be provided by comparison between the selected matrix elements of GF computed at the different theoretical levels. Quite interesting is the case of the GF elements assigned to farthest-distance sites, say μ and ν (the sites are shown explicitly in Fig. 1). The respective GF elements $(G_0)_{\mu\nu}$ will be denoted by G_{far}. The G_{far} values are displayed in Table 3. The latter shows that G_{far} in the CC schemes, as well as in EQC, are sufficiently close to the FCI results. Only the TB values of G_{far} are unreliable, especially for quinoid systems **6** and **7**.

Table 3. The GF matrix elements G_{far} at the various theoretical levels. Bold-font integers refer to the calculated structures from Fig. 1 where the far contact sites are shown

No	TB	EQC	CCD	LCCDm	LCCD2
1	0.396	0.064	0.028	0.029	0.028
2	0.210	0.068	0.026	0.027	0.027
3	0.384	0.064	0.030	0.032	0.032
4	0.670	0.052	0.046	0.046	0.046
5	2.513	0.056	0.062	0.052	0.056
6	0.975	0.089	0.136	0.122	0.127
7	1.254	0.105	0.176	0.155	0.163

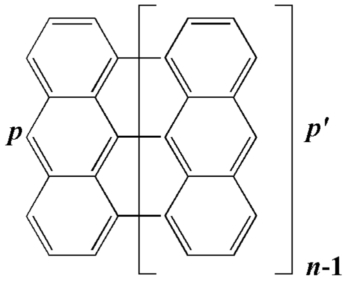

Fig. 2. Structure and the para far-distance contact pair (*p*,*p'*) for [*n*]perianthracene.

6. Green's functions for some conjugated nanostructures

In this section, some results of the π-electron GF computations for sufficiently large conjugated graphene-like molecules are reported. We start with several structures of the previously studied [*n*]periacene systems [8, 9]. Here we consider the perianthracene molecules which are depicted on Fig. 2 with pointing out the most important para-type contact pairs. The numerical results for [*n*]perianthracene structures (Table 4) demonstrate that GF values for the para contacts behave consistently, showing decrease of $(-G_0^X)_{p,p'}$ with distance between sites *p* and *p'*. Only the TB model displays an opposite (unnatural) length dependence.

It is worth noting that, as seen from Table 4, our simplified CC schemes provide the numerical results that are sufficiently close to the CCD ones. This fact allows us to apply LCCDm and LCCD2 for obtaining π-electron GF with certainty, but of course with stipulating that the standard single reference CC theory is correct in principle for the system under study. As usual, medium-size gra-

Table4. Comparison of the para π-electron GF elements $(-G_0^X)_{p,p'}$ in [n]perianthracene (n=1÷3) for X=TB, HPHF, EQC, CCD, LCCDm, and LCCD2

n	TB	HPHF	EQC	CCD	LCCDm	LCCD2
1	1.000	0.626	0.587	0.620	0.614	0.615
2	1.500	0.387	0.366	0.368	0.345	0.350
3	2.500	0.243	0.285	0.294	0.235	0.255

Table 5. Comparison of the far-distance GF elements $(G_0^X)_{p,p'}$ for X = TB, HPHF, EQC, LCCDm, and LCCD2 in GQD-56 and GQD-62

System	(*p,p'*)	TB	HPHF	EQC	LCCD2	LCCDm
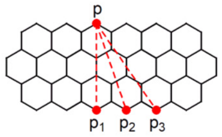	(p,p1)	-2.619	-0.246	-0.399	-0.363	-0.404
	(p,p2)	2.381	0.131	0.283	0.252	0. 292
	(p,p3)	-0.921	-0.036	-0.125	-0.152	-0.126
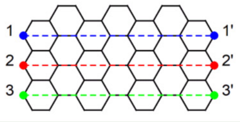	(1,1')	-0.292	-0.051	-0.044	0.038	0.038
	(2,2')	-0.921	-0.155	-0.125	-0.108	-0.108
	(3,3')	-0.615	-0.098	-0.084	-0.070	-0.070

phene molecules having not too small orbital gap are of this structural class.

We now further study two graphene quantum dots GQD-56 and GQD-62 from [9] as additional examples of π-electron nanosystems with rather strong electron correlation effects. The respective data for the most important far-distance elements of GF are collected in Table 5. First, one can immediately notice that again TB gives quantitatively and sometimes even qualitatively erroneous results. More important for our present purposes, there is a close proximity between the LCCDm, LCCD2, and EQC values of far-distant (more sensitive) GF matrix elements (see also Table 6). It indicates that the EQC method as being incomparably more simple in practice, can be more or less safely extended to large-size π-electron structures for which the standard CCD and even LCCD are actually not feasible. As to HPHF, we cannot recommend its application to too large-scale systems because of lacking size-consistency and violating spin conservation in this model.

7. Conclusion

In this work, the approximate computational techniques are proposed for ground-state properties of many-electron π-systems in sufficiently large conjugated molecules. The stress is laid on a good account for π-electron correlation effects needed for considering one-electron Green functions of carbon containing nano-sized structures. Our modified CC π-models present a good basis for producing GF matrices that were computed here in a simple (Koopmans-like) and quite efficient technique. The new approximations, LCCD2 and LCCDm, show a good performance, and as a rule they can be recommended for practical applications.

Particularly, the given models allowed us to evaluate the validity of the previously proposed EQC scheme [8] for medium-size molecular systems. Based on this, we suggest that EQC (which is especially simple in its nature) provides a reasonable description of far-distance GF matrix elements in large conjugated networks. At the same time, the traditional CC theories on which we mainly relied in this study, are not quite infallible for strongly correlated π-systems. In such difficult cases, more specialized approaches should be used, such as the Brueckner coupled cluster theory [13] or spin-flip CC methods [20]. It seems most likely that these advanced CC methods might be a promising area of further researches in molecular electronics.

At last, the present work can be readily extended to the LCCSD-type models as being closely related to the starting model LCCD. Indeed, for molecules with closed shell ground states, a contribution of single excitations has an insignificant influence on most of electronic properties, and we can modify LCCSD in the same fashion as in the case of LCCD. It means that in the corresponding LCCSD equations, the modified correlation potential $g^{(t)}_{corr}$, Eq. (15), can be directly used instead of the initial standard g_{corr}. Preliminary numerical experiments confirm this assumption. Notice that accounting for single excitations, all the same, improves the description of some electronic characteristics, e. g., electric properties, and this issue requires more work and careful consideration in future researches.

Appendix: Quadratic correction to LCCD equations

The simple quadratic correction, Eq. (15), to LCCD can be set up heuristically, following partially the ideas from the previous study in Section C of [21] and in [22].

Table 6. Comparison of the far-distance GF elements $(G_0^X)_{p,p'}$ for X = TB, HPHF, EQC, and LCCDm in dodecahelicene and in short (C_{70}) armchair carbon nanotube CNT (5,0). The π-sites in contact pairs of three distinct types are connected by red, green and blue dashed lines

System	contacts	TB	HPHF	EQC	LCCD2
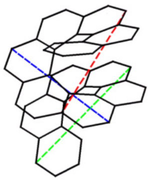	red	-0.104	-0.044	-0.051	-0.038
	green	0.146	0.051	0.061	0.042
	blue	-0.276	-0.124	-0.145	-0.109
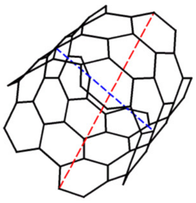	red	0.188	0.052	0.051	0.041
	blue	-0.085	-0.062	-0.064	-0.055

Let us shortly analyze the CCD solution for a two-electron system in two-orbital minimal basis. In this case the CCD solution is equivalent to the FCI solution, as well as to the CID one (a singly excited configuration can by safely neglected). Then the total normalized two-electron function $|\Psi(1,2)|$ can be presented by the two-term expansion as follows:

$$|\Psi(1,2)\rangle = (|\Phi\rangle + t_*|\Phi_{**}\rangle)/\sqrt{1+t_*^2}, \qquad \text{(A1)}$$

where $|\Phi\rangle$ is the corresponding Slater determinant, and $|\Phi_{**}\rangle$ is a doubly excited configuration, with coefficient t_* being a variational parameter.

Take into account that the CID eigenvalue problem allows to be given in the superoperator terms similar to those of the LCCD equation (12). Explicitly,

$$\Pi^{[2]}(t) + g_{corr} = \varepsilon_{corr}t, \qquad \text{(A2)}$$

where the eigenvalue (electron correlation energy)

$$\varepsilon_{corr} = \mathrm{Tr}(g_{corr})^{+}t \equiv \mathrm{Tr}gt. \qquad \text{(A3)}$$

The CID equations (A2) and (A3) are exact for the above $|\Psi(1,2)\rangle$ since they are equivalent to the FCI ones. More generally, exchange terms should be included in ε_{corr}, but they are immaterial for our purpose here.

We now come back to wave function (A1) for which, in concordance with Eq. (53) in [22], the t matrix is equivalent to the rank-one operator

$$t = t_*|\Phi_{**}\rangle\langle\Phi|. \qquad \text{(A4)}$$

In the same manner, g_{corr}, Eq. (13), takes the similar rank-one dyadic form, that is, g_{corr} is of the form of Eq. (A4) where t_* is to be replaced with the relevant element, say g_*. Then, from Eq. (A3) we have $\varepsilon_{corr} = t_*g_*$. Likewise, $\Pi^{[2]}(t) = \lambda_*t$, where λ_* is a double-excitation energy for transition $|\Phi\rangle \to |\Phi_{**}\rangle$. When combined with Eq. (A2), the above relations lead to the scalar equation for parameter t_*:

$$\lambda_*t_* + g_* - t_*g_*t_* = 0, \qquad \text{(A5)}$$

which produces the known solution to the FCI two-electron problem in the minimal basis:

$$t_* = (\lambda_*/g_* - \sqrt{4 + (\lambda_*/g_*)^2})/2,$$

$$\varepsilon_{corr} = (\lambda_* - \sqrt{\lambda_*^2 + 4g_*^2})/2.$$

In operator terms Eq. (A5) is but

$$\Pi^{[2]}(t) + g_{corr} - \mathrm{t}g\mathrm{t} = 0 \qquad \text{(A6)}$$

for the current two-electron problem. The last step we do is merely making a straightforward extension of this rank-one operator equation to a general case of arbitrary molecular system in its singlet ground state, and it gives us the resulting Eqs. (14) and

(15). This is the proposed LCCD2 approximation. The intuitive grounds for such extension can be found in a rather bona-fide electron pair models of the APSG (antisymmetrized product of strongly orthogonal geminals) quality; see also extension of APSG in [23, 24]). In this case the total many-electron function can be thought as being made of actually independent two-electron functions, and for each of them we can apply own equation of type (A6). In other words, due the size consistency of Eqs. (14) and (15) we produce a correct APSG limit when splitting the total closed-shell wave function into a product of wave functions of two-electron fragments. In particular, if a conjugated molecule fully dissociates into isolated ethylene-like fragments, Eqs. (14) and (15) lead to correct π-results of the FCI quality.

The specific computations of ε_{corr} in Section 4 show good results for typical small ($N \le 14$) π-systems treated at the LCCD2 level (see Table 1 in Section 4). For larger N's, there is a simple possibility to compare the approximate ε_{corr} correlation energies with those of the FCI method if we make using the Hubbard Hamiltonian, as done in [18, 25]. In particular, one can extract the needed data from Table 8 in [18], taking, say, the C–C bond resonance integral $\beta_0 = -3$ eV, and the one-center Coulomb integral $\gamma_0 = 5$ eV. With these π-parameters for the cyclic polyene $C_{18}H_{18}$ we have the following $\bar{\varepsilon}_{corr}$ values at the FCI, LCCD2, LCCD and CCD levels (all quantities in eV): −0.1446, −0.1455, −0.1480, −0.1431. Analogous data for $C_{26}H_{26}$ are as follows: −0.1450, −0.1459, −0.1485, −0.1431.

References

1. D.A.Ryndyk, Theory of Qquantum Transport at Nanoscale: An Introduction, Springer, Cham (2016).
2. S.Datta, Lessons from Nanoelectronics. A New Perspective on Transport, World Scientific (2017).
3. J.C.Cuevas, E.Scheer, Molecular Electronics: An Introduction to Theory and Experiment, World Scientific, Singapore (2017).
4. K.H.Khoo, Y.Chen, S.Li, S.Y.Quek, *Phys. Chem.Chem.Phys.*, **17**, 77 (2015).
5. E.P.Hoy, D.A.Mazziotti, T.Seideman, *J.Chem. Phys.*, **147**, 184110 (2017).
6. Y.Tsuji, E.Estrada, R.Movassagh, R.Hoffmann, *Chem.Rev.*, **118**, 4887 (2018).
7. A.V.Luzanov, *Funct.Mater.*, **26**, 152 (2019).
8. A.V.Luzanov, *Funct.Mater.*, **27**, 147 (2020); A.V.Luzanov, in: Nanomaterials and Nanocomposites, Nanostructure Surfaces, and Their Applications. Springer Proc. *Physics*, **246**, ed. by O.Fesenko, L.Yatsenko, Springer, Cham (2021) p.587.
9. A.V.Luzanov, in: Nanooptics, Nanophotonics, Nanostructures, and Their Applications. Springer Proc. in Physics, vol. 222, ed. by O.Fesenko, L.Yatsenko, Springer, Cham (2019), p.341.
10. B.T.Pickup, O.Goscinski, *Mol.Phys.*, **26**, 1013 (1973).
11. M.Nooijen, J.G.Snijders, *Int.J.Quantum Chem.*, **48**, 15 (1993).
12. M.Nooijen, J.G.Snijders, *J.Chem.Phys.*, 102, 1681 (1995).
13. I.Shavitt, R.J.Bartlett, Many-body Methods in Chemistry and Physics: MBPT and Coupled-cluster Theory, Cambridge University Press (2009).
14. K.Bhaskaran-Nair, K.Kowalski, W.A.Shelton, *J.Chem.Phys.*, **144**, 144101 (2016).
15. A.V.Luzanov, *J.Struct.Chem.*, **44**, 681 (2003).
16. K.G.L.Pedersen, M.Strange, M.Leijnse et al., *Phys.Rev.B*, **90**, 125413 (2014).
17. A.B.Zakharov,V.V.Ivanov, *J.Struct.Chem.*, **52**, 645 (2011); A.B.Zakharov, V.V.Ivanov, L.Adamowicz. in: Practical Aspects of Computational Chemistry IV, ed. by J.Leszczynski, M.K.Shukla, Springer, New York (2016), p.57.
18. J.Paldus, M.Takahashi, R.W.H.Cho, *Phys. Rev.B*, **30**, 4267 (1984).
19. A.V.Luzanov, Y.F.Pedash. *Theor.Experim. Chem.*, **21**, 367 (1976); A.V.Luzanov, *Int.J. Quantum Chem.*, **108**, 671 (2008).
20. D.Casanova, A.I.Krylov, *Phys.Chem.Chem. Phys.*, **22**, 4326 (2020).
21. A.V.Luzanov, O.V.Prezhdo, *J.Chem.Phys.*, **124**, 224109 (2006).
22. A.V.Luzanov, O.V.Prezhdo, *J.Chem.Phys.*, **125**, 154106 (2006).
23. V.A.Rassolov, *J.Chem.Phys.*, **117**, 5978 (2002).
24. E.Pastorczak, K.Pernal, *Phys.Chem.Chem. Phys.*, **17**, 8622. (2015).
25. K.Hashimoto, J.Cizek, J.Paldus, *Int.J.Quantum.Chem.*, **34**, 407 (1988).